

## ELASTIC INSTABILITY AND NONLINEAR ANALYSIS OF THIN-WALLED MEMBERS UNDER NON-CONSERVATIVE FORCES

*By Akio HASEGAWA\*, Toru MATSUNO\*\* and Fumio NISHINO\*\*\**

Elastic instability and the nonlinear finite displacement behavior for spatial thin-walled members under displacement-dependent loads are investigated. The displacement-dependency is reflected on the load stiffness matrix, of which the nonsymmetry indicates the nonconservative loads. A general formulation to derive the load stiffness matrix is presented. As important examples, the follower force and the wind forces are treated, and their load stiffness matrices are given explicitly. The mass matrix of thin-walled members is also derived to examine the dynamic instability. The nonlinear finite element analysis as well as the static and dynamic instability analyses are made as computational examples for the follower force and the wind forces, and some interesting features are discussed.

*Keywords:* Static Instability, Dynamic Instability, FEM, Nonlinear Analysis, Thin-Walled Members, Follower Force, Wind Forces

### 1. INTRODUCTION

In the common structural stability analysis, the external forces considered are mainly the gravity loadings such as the live and dead loads. The direction of the gravity loadings does not depend on displacements during the deformations of the structures. However, the direction of external loads in the real situation may be changed and displacement-dependent such as water pressure or wind forces. But in the standard and practical analysis, the method has been simplified and load is kept constant during the deformation. Even if the displacement-dependency of the loads is considered, the analysis method has been either abstract, mathematically complicated or treated in an approximate manner, mostly concerning the determination of the critical loads for simple hypothetical structures, and the general method for numerical computation has not been well established yet, particularly for the instability and nonlinear finite displacement behavior of spatial structures, although some literature are available as general references 1)~4) and as specific papers for the FEM analysis<sup>5),6)</sup> and the theoretical investigation<sup>7)</sup>. The purpose of this paper is to develop a general and efficient analysis method for the elastic stability and the finite displacement behavior of thin-walled space structures under the displacement-dependent loads, using the finite element technique. The general tangential stiffness equation to analyze thin-walled spatial structures including warping contribution has been given in Reference 8) for the displacement-independent loadings only. As a natural consistent extension to include the effects of the displacement-dependency of external loads, the theorem of virtual work for linearized finite displacements is established and the

\* Member of JSCE, Dr. Eng., Associate Professor, Division of Structural Engineering and Construction, Asian Institute of Technology (G. P. O. Box 2754, Bangkok 10501, Thailand) on leave from Univ. of Tokyo.

\*\* Mr. Eng., Ohbayashi-Gumi Co. Ltd., formerly Graduate Student, Department of Civil Engineering, Univ. of Tokyo (Bunkyo-ku, Tokyo).

\*\*\* Member of JSCE, Ph. D., Professor, Department of Civil Engineering, Univ. of Tokyo (Bunkyo-ku, Tokyo)

tangential stiffness equation of the thin-walled members is developed for the problems of displacement-dependent loadings.

The displacement-dependent loads do not always have potentials, depending on the nature of displacement-dependency of the loads. If external loads have potentials, they are called conservative forces, otherwise, nonconservative forces. The conservativeness of external loads can be checked by symmetry of the load stiffness matrices, as indicated in References 5) ~7). For the conservative loading, the load stiffness matrices derived from displacement-dependency of the loads are symmetric. But for the nonconservative loadings, those matrices are nonsymmetric. This criterion for the conservativeness of the loads seems important particularly on the numerical analysis of elastic stability. Although the conservative loads always produce the static instability only, the nonconservative loads may create the static instability called divergence and/or the dynamic instability called flutter, depending on the type of problems and the magnitude of parameters concerned. Hence, in this paper, the mass matrix of spatial thin-walled members is also derived to examine the dynamic instability.

Finally, illustrative examples using the tangential stiffness equation derived in this study are presented. Two examples of displacement-dependent loads are considered. One is the problem of cantilever column subjected to follower force which is frequently quoted as an example of displacement-dependent loads<sup>9)</sup>. The other is the problem of wind forces acting on thin-walled beams which is treated as a typical example for the spatial behavior of thin-walled structures. The elastic stability and finite displacement behaviors are of primary concern. For the numerical examples for those purposes, four types of analysis methods are used. The first is the common static stability analysis. The second is the dynamic stability analysis involving the mass matrix to examine a possibility of the dynamic instability, whatever the static instability exists for the nonconservative loads or not. The third is the nonlinear finite displacement analysis, and the last one is the linearized finite displacement analysis which is expected to be very simple and effective for practical engineering applications, both of which (the third and the fourth) are applied for static instability of nonconservative systems. Through the above analyses, the versatility and the validity of the present formulations are demonstrated.

## 2. STIFFNESS EQUATION OF THIN-WALLED MEMBERS UNDER DISPLACEMENT-DEPENDENT LOADS

The general stiffness equation of spatial thin-walled members developed in Reference 8) does not consider the displacement-dependency of the loads. Hence, by using the theorem of virtual work for the linearized finite displacement theory, the stiffness equation of thin-walled members applicable for the problems of the displacement-dependent loads is derived. In this derivation, the kinematic field and notations of thin-walled members are based on Reference 8) (see Fig. 1).

The virtual work equation with body forces for general continua with volume  $V$  and surface  $S$  can be expressed in the form

$$\int_V (\bar{\sigma}_{ij} \delta \bar{e}_{ij}) dV - \int_V (\bar{p}_i \delta \bar{u}_i) dV - \int_S (\bar{T}_i \delta \bar{u}_i) dS = 0 \dots\dots\dots (1)$$

in which  $\bar{\sigma}_{ij}$  and  $\bar{e}_{ij}$  are the second Piola-Kirchhoff's stress tensor and Green's strain tensor respectively, and  $\bar{p}_i$  and  $\bar{T}_i$  are body forces and surface forces acting on the continuum respectively, and  $\bar{u}_i$  are displacements caused by these forces.

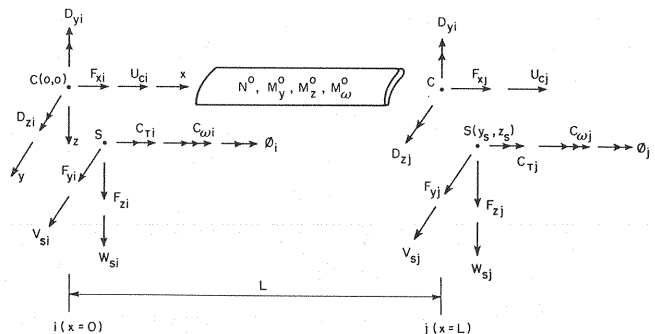


Fig. 1 Generalized Forces and Displacements.

At the reference state defined as  $u_i^0=0$ , the system is supposed in equilibrium under  $\sigma_{ij}^0$ ,  $p_i^0$  and  $T_i^0$ . Considering that the system is also in equilibrium after the application of incremental surface forces (loads at the nodal points), body forces and corresponding displacements, the following components, which take the effects of the displacement-dependency of external forces into consideration, are introduced as

$$\left. \begin{aligned} \bar{\sigma}_{ij} &= \sigma_{ij}^0 + \sigma_{ij}^L + \sigma_{ij}^{NL} & \bar{e}_{ij} &= e_{ij}^L + e_{ij}^{NL} & \bar{u}_i &= u_i \\ \bar{p}_i &= p_i^0 + p_i + p_i^{0L} + p_i^L + p_i^{NL} & \bar{T}_i &= T_i^0 + T_i + T_i^{0L} + T_i^L + T_i^{NL} \end{aligned} \right\} \dots\dots\dots (2 \text{ a-e})$$

The superscript '0' denotes values at the reference state, and 'L' and 'NL' are linear and nonlinear parts of quantities measured from the reference state.  $p_i$  and  $T_i$  express the increments of loads, the directions of which are the same as those at the reference state.  $p_i^{0L}$  and  $T_i^{0L}$  are the linear components produced by the displacement-dependency of the loads at the reference state.  $(p_i^L, T_i^L)$  and  $(p_i^{NL}, T_i^{NL})$  are the linear and nonlinear components produced by the displacement-dependency of the incremental loads, both of which can be treated as the second and higher order small quantities.

Substituting Eqs. (2) into Eq. (1) and neglecting the third and higher order quantities, the virtual work equation can be written in the form

$$\int_V (\sigma_{ij}^0 \delta e_{ij}^{NL} + \sigma_{ij}^L \delta e_{ij}^L + \sigma_{ij}^L \delta e_{ij}^L) dV - \int_V (p_i^0 \delta u_i + p_i \delta u_i + p_i^{0L} \delta u_i) dV - \int_S (T_i^0 \delta u_i + T_i \delta u_i + T_i^{0L} \delta u_i) dS = 0 \dots\dots\dots (3)$$

Taking into consideration that the system is in equilibrium in terms of small displacements for the reference state which is before the application of the incremental loads, as expressed by

$$\int_V (\sigma_{ij}^0 \delta e_{ij}^L) dV - \int_V (p_i^0 \delta u_i) dV - \int_S (T_i^0 \delta u_i) dS = 0 \dots\dots\dots (4)$$

Eq. (3) is reduced to the equation as

$$\int_V (\sigma_{ij}^0 \delta e_{ij}^{NL} + \sigma_{ij}^L \delta e_{ij}^L) dV - \int_V (p_i \delta u_i + p_i^{0L} \delta u_i) dV - \int_S (T_i \delta u_i + T_i^{0L} \delta u_i) dS = 0 \dots\dots\dots (5)$$

in which  $p_i^{0L}$  and  $T_i^{0L}$  indicate the displacement-dependency of the reference loads and they are the first order quantities of displacements. By using arbitrary displacement  $u_j$  and arbitrary nodal displacement  $U_j$ , those quantities can be expressed as

$$p_i^{0L} = t_{ij} u_j \quad T_i^{0L} = s_{ij} U_j \dots\dots\dots (6 \text{ a, b})$$

in which  $t_{ij}$  and  $s_{ij}$  are coefficients which may depend on the continuously changing deformed configuration of the reference state. Substituting Eqs. (6) into Eq. (5), assuming that  $t_{ij}$  and  $s_{ij}$  are independent from integration, Eq. (5) yields

$$\int_V (\sigma_{ij}^0 \delta e_{ij}^{NL} + \sigma_{ij}^L \delta e_{ij}^L) dV - t_{ij} \int_V (u_j \delta u_i) dV - s_{ij} \int_S (U_j \delta U_i) dS - \int_V p_i \delta u_i dV - \{F\}^T \delta \{d\} = 0 \dots\dots\dots (7)$$

where  $\{F\}$  is the nodal force vector, and  $\{d\}$  is the corresponding displacement vector, as given for spatial thin-walled members by

$$\{F\} = \{F_x\}^T, \{F_y\}^T, \{F_z\}^T, \{T\}^T \quad \{d\} = \{u\}^T, \{v\}^T, \{w\}^T, \{\phi\}^T \dots\dots\dots (8 \text{ a, b})$$

where

$$\left. \begin{aligned} \{F_x\} &= \{F_{xi}, F_{xj}\}^T & \{F_y\} &= \{F_{yi}, D_{yi}, F_{yj}, D_{yj}\}^T \\ \{F_z\} &= \{F_{zi}, D_{zi}, F_{zj}, D_{zj}\}^T & \{T\} &= \{C_{Ti}, C_{\omega i}, C_{Tj}, C_{\omega j}\}^T \end{aligned} \right\} \dots\dots\dots (9 \text{ a-d})$$

and

$$\left. \begin{aligned} \{u\} &= \{u_{ci}, u_{cj}\}^T & \{v\} &= \{v_{si}, -v'_{si}, v_{sj}, -v'_{sj}\}^T \\ \{w\} &= \{w_{si}, -w'_{si}, w_{sj}, -w'_{sj}\}^T & \{\phi\} &= \{\phi_i, -\phi'_i, \phi_j, -\phi'_j\}^T \end{aligned} \right\} \dots\dots\dots (10 \text{ a-d})$$

in which the displacement components with subscripts  $i$  and  $j$  refer to the cross-section at  $x=0$  and  $L$  respectively, as shown in Fig. 1.

At this stage, the following set of the well-known interpolation functions is introduced as

$$\left. \begin{aligned} N_1 &= 1 - (x/L) & N_2 &= (x/L) \\ N_3 &= 1 - 3(x/L)^2 + 2(x/L)^3 & N_4 &= -x + 2(x^2/L) - (x^3/L^2) \\ N_5 &= 3(x/L)^2 - 2(x/L)^3 & N_6 &= (x^2/L) - (x^3/L^2) \end{aligned} \right\} \dots\dots\dots (11 \text{ a-f})$$

and the displacement components at an arbitrary cross-section ( $0 \leq x \leq L$ ) can be written in terms of the nodal displacements as

$$u_c = \{A\}^T \{d\} \quad v_s = \{B_1\}^T \{d\} \quad w_s = \{B_2\}^T \{d\} \quad \phi = \{B_3\}^T \{d\} \dots (12 \text{ a-d})$$

where

$$\left. \begin{aligned} \{A\} &= \{N_1, N_2, 0, 0, 0, 0, 0, 0, 0, 0, 0, 0, 0, 0\}^T \\ \{B_1\} &= \{0, 0, N_3, N_4, N_5, N_6, 0, 0, 0, 0, 0, 0, 0, 0\}^T \\ \{B_2\} &= \{0, 0, 0, 0, 0, 0, N_3, N_4, N_5, N_6, 0, 0, 0, 0\}^T \\ \{B_3\} &= \{0, 0, 0, 0, 0, 0, 0, 0, 0, 0, N_3, N_4, N_5, N_6\}^T \end{aligned} \right\} \dots (13 \text{ a-d})$$

From Eqs. (12) and (13), an arbitrary displacement  $u_i$  can be re-expressed as

$$u_i = \{C_i\}^T \{d\} \dots (14)$$

in which  $\{C_i\}$  is the interpolation functions corresponding to displacement  $u_i$ , obtainable from Eq. (13).

And, an arbitrary nodal displacement  $U_i$  is also re-expressed as

$$U_i = \{D_i\}^T \{d\} \dots (15)$$

in which  $\{D_i\}$  is the vector of 14 dimensions, where only the component corresponding to  $U_i$  is equal to 1 and the others equal to 0.

Noting the kinematic and stress fields of thin-walled members at the reference state<sup>9)</sup>, substituting Eqs. (11) (14) and (15) into Eq. (7) leads to the general stiffness equation of a thin-walled beam applicable for the displacement-dependent loads, as expressed by

$$\{F\} = (K_T + K_V + K_S) \{d\} - \{F_0\} \dots (16)$$

in which  $K_T$  is the tangential stiffness matrix including geometrical stiffness already given explicitly in Ref. 8).  $K_V$  is the load stiffness matrix produced by the displacement-dependency of distributed loads, as expressed by

$$K_V = -t_{ij} \int_0^L \{C_i\} \{C_j\}^T dx \dots (17)$$

$K_S$  is the load stiffness matrix produced by the displacement-dependency of nodal loads, as expressed by

$$K_S = -s_{ij} \{D_i\} \{D_j\}^T \dots (18)$$

and  $\{F_0\}$  is the equivalent nodal force vector resulting from the displacement-independent incremental distributed forces.

### 3. LOAD STIFFNESS MATRIX OF FOLLOWER FORCE

The problem of the so-called follower force is shown in Fig. 2; where a constant compressive force  $P$  is applied to the column and always acts in the direction of the tangent to the deflection curve at the top of the column. This problem is examined here as an example of displacement-dependent nodal loads, and its load stiffness matrix is derived. For this inplane problem, the nodal force vector and the displacement vector are extracted from Eq. (8), as expressed by

$$\{F\} = \{F_x\}^T, \{F_z\}^T \quad \{d\} = \{u\}^T, \{w\}^T \dots (19 \text{ a, b})$$

As shown in Fig. 2, the nodal incremental loads  $T_i^{0L}$  resulting from the displacement-dependency at the deformed configuration are given by

$$F_{xj} = -(P^0 + P) \cos \lambda + (P^0 + P) \quad F_{zj} = -(P^0 + P) \sin \lambda \dots (20 \text{ a, b})$$

Assuming that  $\cos \lambda \doteq 1$  and  $\sin \lambda \doteq \lambda$  with  $\lambda = -w'$ , Eq. (20) is reduced to

$$F_{xj} = 0 \quad F_{zj} = -(P^0 + P)(-w') \dots (21 \text{ a, b})$$

Noting that the term  $Pw'$  is negligible because of its higher order quantity, substituting Eqs. (21) into Eq. (18), by making use of Eqs. (6) and (15), leads to the load stiffness matrix of follower force as

$$K_S = P^0 \{D_0\} \{D_1\}^T \dots (22)$$

where

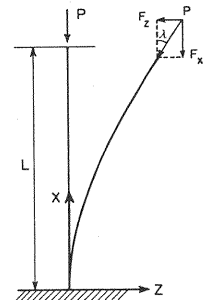


Fig. 2 Follower Force.

$$\{D_0\} = \{0, 0, 0, 0, 1, 0\}^T \quad \{D_1\} = \{0, 0, 0, 0, 0, 1\}^T \dots \dots \dots (23 \text{ a, b})$$

and thus, the load stiffness matrix  $K_s$  is given explicitly as

$$K_s = P^0 \begin{bmatrix} 0 & 0 & 0 & 0 & 0 & 0 \\ 0 & 0 & 0 & 0 & 0 & 0 \\ 0 & 0 & 0 & 0 & 0 & 0 \\ 0 & 0 & 0 & 0 & 0 & 0 \\ 0 & 0 & 0 & 0 & 0 & 1 \\ 0 & 0 & 0 & 0 & 0 & 0 \end{bmatrix} \dots \dots \dots (24)$$

#### 4. LOAD STIFFNESS MATRIX OF WIND FORCES

The load stiffness matrix of wind forces is developed here as an example of the displacement-dependent distributed loads. The treatment of wind forces is based on Ref. 10). It is assumed that constant wind velocity  $U$  is applied to the beam perpendicularly to the axis. In the analysis, static wind forces are decomposed into three force components across the section, namely drag, lift, and moment, as shown in Fig. 3. They are expressed with aerodynamic coefficients  $C_D$ ,  $C_L$ ,  $C_M$  respectively as

$$p_z = C_D A q \quad p_y = C_L b q \quad C = C_M b^2 q \dots \dots \dots (25 \text{ a-c})$$

in which  $A$  and  $b$  are the depth and width of the beam section,  $q$  is the wind pressure expressed with air density  $\rho$  and wind velocity  $U$  as

$$q = (1/2) \rho U^2 \dots \dots \dots (26)$$

Generally, aerodynamic coefficients are not constant during the deformation, but depend on the angle of yaw  $\phi$ . It is now assumed that the gradients of aerodynamic coefficients are given by  $s_D$ ,  $s_L$  and  $s_M$  at the reference state with  $q_0$ . Then considering that the system is in

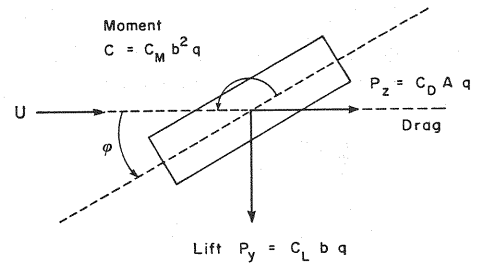


Fig. 3 Wind Forces.

equilibrium after the application of wind pressure increment  $q$  and corresponding displacement increment  $\phi$ , the incremental distributed loads at the deformed configuration are given by

$$p_z = s_D A (q^0 + q) \phi \quad p_y = s_L b (q^0 + q) \phi \quad C = s_M b^2 (q^0 + q) \phi \dots \dots \dots (27 \text{ a-c})$$

in which the term  $q\phi$  is negligible because of its higher order quantity. Substituting Eqs. (27) into Eq. (17) by making use of Eqs. (6) and (14), the load stiffness matrix of wind forces is obtained as

$$K_v = -s_L b q^0 \int_L \{B_1\} \{B_3\}^T dx - s_D A q^0 \int_L \{B_2\} \{B_3\}^T dx - s_M b^2 q^0 \int_L \{B_3\} \{B_3\}^T dx \dots \dots \dots (28)$$

which is expressed explicitly as

$$K_v = - \begin{bmatrix} 0 & 0 & 0 & 0 \\ 0 & 0 & 0 & s_L b K_w \\ 0 & 0 & 0 & s_D A K_w \\ 0 & 0 & 0 & s_M b^2 K_w \end{bmatrix} \quad K_w = q^0 L / 420 \begin{bmatrix} 156 & & & \\ -22 L & 4 L^2 & & \\ 54 & -13 L & 156 & \\ 13 L & -3 L^2 & 22 L & 4 L^2 \end{bmatrix} \text{Sym.} \dots \dots \dots (29 \text{ a, b})$$

#### 5. MASS MATRIX OF THIN-WALLED MEMBERS

In order to examine the dynamic instability, the stiffness equation of small vibration of thin-walled members is derived in this chapter. Considering that the inertia forces by movements represent body forces, the virtual work equation is expressed as

$$\int_V (\bar{\sigma}_{ij} \delta \bar{e}_{ij}) dV - \int_V (\bar{p}_i \delta \bar{u}_i) dV - \int_S (\bar{T}_i \delta \bar{u}_i) dS - \int_V (\rho_m \ddot{u}_i \delta \bar{u}_i) dV = 0 \dots \dots \dots (30)$$

in which  $\rho_m$  is the mass density of the material, and  $(\cdot)$  denotes differentiation with respect to time. The 4th term of the left hand side of Eq. (30) is the new additional term to Eq. (1). Applying this virtual work

equation for a thin-walled beam, and considering that the independent displacement components  $\bar{u}$ ,  $\bar{v}$ ,  $\bar{w}$  are quantities at the centroid, and  $\phi$  is a quantity at the shear center, all of which are measured from the reference state, the 4th term of the left hand side of Eq. (30) can be given by

$$\rho_m A \int_L \ddot{u}_c \delta u_c dx + \rho_m A \int_L \ddot{v}_c \delta v_c dx + \rho_m A \int_L \ddot{w}_c \delta w_c dx + \rho_m I_M \int_L \ddot{\phi} \delta \phi dx \dots \dots \dots (31)$$

in which  $I_M$  is the polar moment of inertia referring to the shear center, as expressed by

$$I_M = \int_A \{(y - y_s)^2 + (z - z_s)^2\} dA \dots \dots \dots (32)$$

By using the coordinate system as shown in Fig. 1, displacements  $v_c$  and  $w_c$  are given as

$$v_c = v_s + y_s(1 - \cos \phi) + z_s \sin \phi \quad w_c = w_s - y_s \sin \phi + z_s(1 - \cos \phi) \dots \dots \dots (33 \text{ a, b})$$

Using the Taylor expansion and neglecting the second and higher order terms, Eqs. (33) are reduced to

$$v_c = v_s + z_s \phi \quad w_c = w_s - y_s \phi \dots \dots \dots (34 \text{ a, b})$$

Substituting Eqs. (34) into Eq. (31) leads to

$$\begin{aligned} & \rho_m A \int_L \ddot{u}_c \delta u_c dx + \rho_m A \int_L \ddot{v}_s \delta v_s dx + \rho_m A \int_L \ddot{w}_s \delta w_s dx + z_s \rho_m A \int_L (\ddot{\phi} \delta v_s + \dot{v}_s \delta \dot{\phi}) dx \\ & - y_s \rho_m A \int_L (\ddot{\phi} \delta w_s + \dot{w}_s \delta \dot{\phi}) dx + \rho_m \{I_M + A(y_s^2 + z_s^2)\} \int_L \ddot{\phi} \delta \phi dx \end{aligned}$$

and then substituting this into Eq. (30), by making use of the interpolation functions of Eqs. (12), the stiffness equation of small vibration is obtained as

$$\{F\} = (K_T + K_V + K_S) \{d\} - \{F^0\} + M \{\ddot{d}\} \dots \dots \dots (35)$$

where the mass matrix  $M$  is given explicitly by

$$\begin{aligned} M &= \rho_m L / 420 \left[ \begin{array}{cccc} AK_{m1} & & & \text{Sym.} \\ 0 & AK_{m2} & & \\ 0 & 0 & AK_{m2} & \\ 0 & z_s AK_{m2} & -y_s AK_{m2} & \{I_M + A(y_s^2 + z_s^2)\} K_{m2} \end{array} \right] \\ K_{m1} &= \begin{bmatrix} 140 & 70 \\ 70 & 140 \end{bmatrix} \quad K_{m2} = \begin{bmatrix} 156 & & & \text{Sym.} \\ -22L & 4L^2 & & \\ 54 & -13L & 156 & \\ 13L & -3L^2 & 22L & 4L^2 \end{bmatrix} \end{aligned} \dots \dots \dots (36 \text{ a-c})$$

### 6. ANALYSIS METHOD

Four types of analysis methods are presented herein. The first is the common static stability analysis. The second is the dynamic stability analysis involving the mass matrix to examine a possibility of the dynamic instability. The third and the last are the nonlinear and linealized finite displacement analyses, respectively, both of which are applied for static instability of nonconservative systems.

#### (1) Static method for stability problems

Static stability problems can be solved as an eigen value problem through Eq. (16) by

$$\det [K_E + \lambda \{K_G(N^0) + K_V(q^0) + K_S(P^0)\}] = 0 \dots \dots \dots (37)$$

in which  $q^0$  and  $P^0$  are the displacement-dependent distributed loads and nodal forces at the reference state respectively,  $N^0$  expresses stress resultants, and  $K_E$  is the stiffness of small displacements and  $K_G$  is the geometric stiffness. From this equation, the value of coefficient  $\lambda$  is obtained, and  $\lambda q^0$  or  $\lambda P^0$  is the critical value.

#### (2) Dynamic method for stability problems

The basic eigenvalue equation for the dynamic instability is expressed through Eq. (35) by

$$\det [K_E + \lambda \{K_G(N^0) + K_V(q^0) + K_S(P^0)\} - \omega^2 M] = 0 \dots \dots \dots (38)$$

in which  $\omega$  is the frequency, as introduced by

$$\{d\} = \{f\} e^{i\omega t} \dots \dots \dots (39)$$

in which  $\{f\}$  is the amplitude independent of time, and  $t$  expresses time. If  $\omega$  has a minus imaginary part, the vibration  $\{d\}$  will diverge. So,  $\lambda$  which gives  $\omega$  a minus imaginary part indicates the critical value which is given by  $\lambda q^0$  or  $\lambda P^0$ .

Two types of instabilities are obtainable from Eq. (38). In the case that all the  $\omega^2$  obtained from Eq. (38) are real, the instability occurs when the smallest  $\omega^2$  becomes minus. Then,  $\lambda$  which gives  $\omega^2$  zero is the critical value, and in such a case, Eq. (38) is the same as Eq. (37). This type of the instability is called Static Instability (or Divergence). On the other hand, when  $\omega^2$  has a imaginary part, an instability also occurs. This type of instability can not be obtained from Eq. (37), and this is called Dynamic Instability (or Flutter).

When the load stiffness matrices are symmetric because of the conservativeness of external loads, all the  $\omega^2$  in Eq. (38) are real. So, instabilities caused by conservative forces are always static. However, when the load stiffness matrices are nonsymmetric because of the nonconservativeness of the external loads,  $\omega^2$  may be complex. In such a case, instabilities caused by these forces may be a static instability for the former case, and may be a dynamic instability for the latter.

### (3) Nonlinear finite displacement analysis

The tangential stiffness equation of thin-walled members after the application of the set of incremental loads  $\{F\}$  and  $\{F^0\}$  can be expressed by

$$\{F\} = [K_E(w_n) + K_G(w_n, N^0) + K_V(w_n, q^0) + K_S(w_n, P^0)] \{d\} - \{F^0\} \quad (40)$$

in which  $w_n$  refers to the geometrical configuration at the reference state for the formation of the stiffness matrix, and  $N^0$  expresses the stress resultants, and  $q^0$  and  $P^0$  are the external loads at the reference state. In the analysis, a non-iterative computational scheme<sup>11)</sup> is used to trace the exact nonlinear finite displacement behavior of thin-walled members.

### (4) Linearized finite displacement analysis

This method assumes that  $w_n$  of Eq. (40) always refers to the initial configuration  $w_0$  for the formation of stiffness matrix, and is not updated as in the nonlinear finite displacement analysis. The displacement  $\{d\}$  which is the accumulated value from the initial configuration is calculated by applying a set of the accumulated loads  $\{F\}$  and  $\{F^0\}$  for the initial configuration with  $N^0$ ,  $q^0$  and  $P^0$  also defined at the initial configuration. This method is very simple and corresponds to the well-known analytical beam-column solution for plane beams, and therefore is expected to be very effective before very large deflection behavior, but still in the range of finite displacements.

## 7. COMPUTATIONAL ILLUSTRATIVE EXAMPLES

### (1) Follower force

First, the instability of a column under follower force, as shown in Fig. 4, is examined by the static and the dynamic methods. By the static method, all the eigenvalues have been found complex and the critical load can not be obtained, indicating that the static instability does not occur. But, through the dynamic method, the critical value of the dynamic instability has been obtained with the frequency  $\omega$  being complex. The computed results are compared with the available results from Ref. 9), as given in Table 1. The results are found to be in good agreement with the existing analytical results.

Next, the nonlinear static finite displacement analysis is performed to obtain the load-displacement behaviors of a column under the follower force and under the conservative constant directional force respectively applied at the free end, with an initial disturbing horizontal load at the same point. The results are shown in Fig. 5, indicating that the follower force does not show divergence and the horizontal displacement returns to zero at the load  $P/P_{cr}=8$  which produces the dynamic instability. Also computed are both of the static and dynamic stability analyses for the partial follower force, that is, the combined case of the follower and constant directional forces. The results are shown in Fig. 6, demonstrating some interesting features of stability phenomena, where either static or dynamic or both of them have been

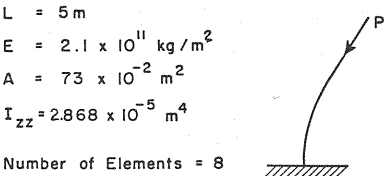


Fig.4 A Cantilever Subjected to Follower Force.

Table 1 Instability of a Cantilever.

k	C.D.F.	F.F.
Ref. 9	0.25	2.008
F.E.M.	0.25	2.030

Note:  $P_{cr} = k\pi^2EI_{zz}/L^2$   
C.D.F. = Constant Directional Force  
F.F. = Follower Force

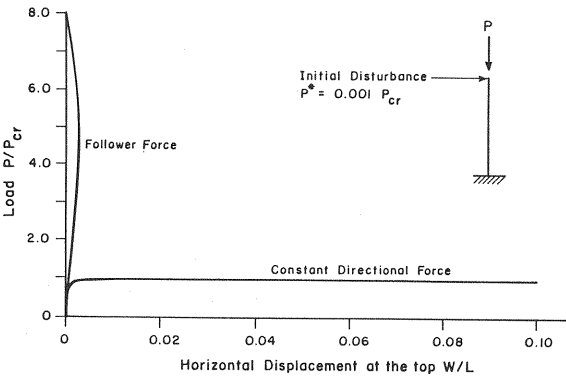


Fig.5 Load-Displacement behavior of a Cantilever.

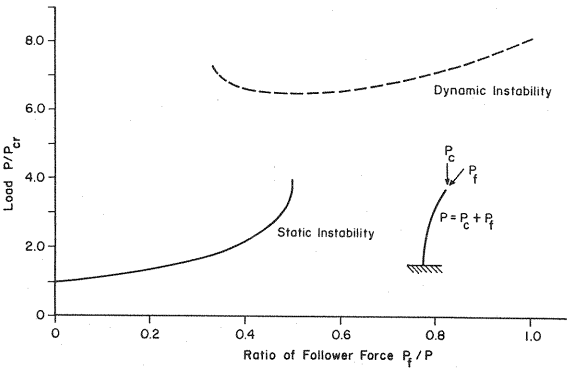


Fig.6 Critical Load of a Cantilever Subjected to Partial Follower Force.

$L = 10\text{ m}$   
 $d/b = 0.20$   
 $E = 2.1 \times 10^{11}\text{ kg/m}^2$   
 $G = 8.1 \times 10^{10}\text{ kg/m}^2$   
 $C_D = 0.28$  for  
 $P_z = C_D b q$  instead of  $C_D A q$   
 $S_L = 2.86$   
 $S_M = -0.47$

Number of Elements = 8

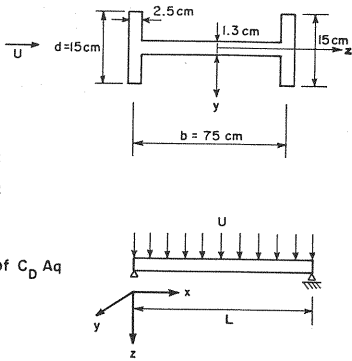


Fig.7 A Simple Beam Under Wind Forces.

observed, depending on the ratio of the follower force.

(2) Wind forces

First, the static instability of a straight symmetric simply supported I beam under the wind forces is examined, as shown in Fig. 7. Here, three types of analyses are examined, the first considers only the drag of the wind force, the second considers the drag and lift, and the last considers all the three aerodynamic forces, i.e. drag, lift and moment. In this example, the aerodynamic coefficient  $C_D$  is assumed always constant, approximating the measured typical aerodynamic force curves for H-sections<sup>10)</sup>. It should be noted that this is different from the assumption of Eq. (27 a), but the force is displacement independent, resulting in the stiffness matrix expression such that  $s_D A K_w$  is reduced to zero matrix in Eq. (29 a), and, instead of this, the drag of Eq. (25 a) is reflected in the equivalent force vector of  $\{F^0\}$  in Eq. (16) or (35), as expressed by  $\int_L p_z \{B_2\} dx$ .  $C_L$  and  $C_M$  are also approximated from the same source<sup>10)</sup> as  $C_D$ , being first equal to 0 for  $\phi=0$ , and changing linearly as the torsion of the beam increases as given by Eqs. (27 b, c) in an incremental form. The results of computations are shown in Table 2, where all the eigenvalues were found real, and it was also confirmed that  $\omega^2$  of the dynamic analysis did not contain the complex values. The computed results are found to be in good agreements with the existing approximate results found in Ref. 10).

For a possible example of dynamic instability, a solution is given in Fig. 8, where the gradient of the lift coefficient  $s_L$  is varied in the vicinity of zero as parameter with the drag coefficient being constant  $C_D=0.28$  and the moment coefficient  $C_M$  neglected to be zero. It is interesting to note that the dynamic



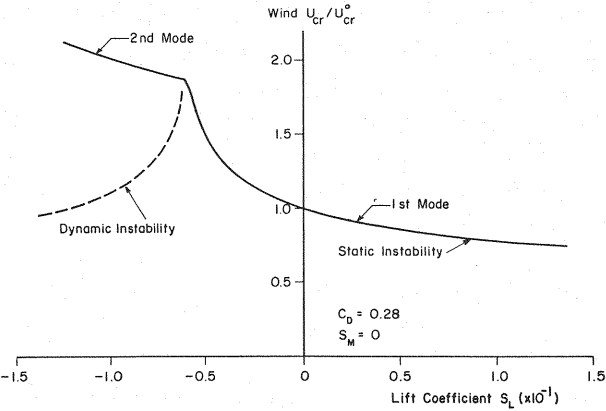


Fig.8 Effects of Lift  $S_L$  on Static and Dynamic Instabilities.

Table2 Instability of a Beam under Wind Forces.

k		1st Mode	2nd Mode
$C_D$	Ref.10	7.48	14.53
	F.E.M.	8.84	15.26
$C_D + S_L$	Ref.10	3.33	7.77
	F.E.M.	3.37	7.83
$C_D + S_L + S_M$	Ref.10	4.21	9.45
	F.E.M.	4.26	9.58

Note:

$$U_{cr}^2 = k \frac{1}{\rho} \frac{1}{bL^2} \sqrt{\frac{\pi^2 EI_{yy}}{L^2} \left( GJ + \frac{\pi^2 EI_{zz}}{L^2} \right)}$$

instability does occur, depending on the value of  $S_L$ , where the characteristics of the static instability change abruptly due to the change of static buckling mode from the first mode to second mode.

Considered next is the load-displacement behavior of the I-beam under the same condition as in Fig. 7. In this case, an initial disturbing  $y$ -directional load is applied at the center of the beam. Fig. 9 shows the behavior of the rotation at the center of the beam under the wind, where the deformation remains relatively small, but finite. These results computed by the nonlinear finite displacement analysis for three cases of wind loadings are compared with the linearized finite displacement analysis as described before. The results obtained by two different methods show a very good agreement, demonstrating a good accuracy of the linearized finite displacement analyses for relatively small but finite displacements near the buckling points. Fig.10 shows the post-buckling behavior of large displacement at the same point of the beam, computed by the nonlinear finite displacement analysis, which is proved to be effective to trace the large deformation for the thin-walled members subjected to displacement-dependent loadings.

8. CONCLUDING REMARKS

Elastic instability and nonlinear finite displacement behavior for spatial thin-walled members under displacement-dependent loadings have been investigated in this paper. When the load is displacement-dependent, the tangential stiffness matrix includes the load stiffness matrix, of which symmetry or nonsymmetry corresponds to conservativeness or nonconservativeness of loadings, respectively.

As a natural and consistent extension from the general tangent stiffness matrix for thin-walled members

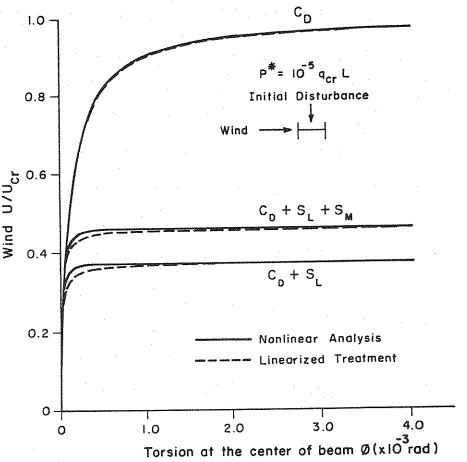


Fig.9 Behavior of a Beam under Wind Forces near Buckling Points.

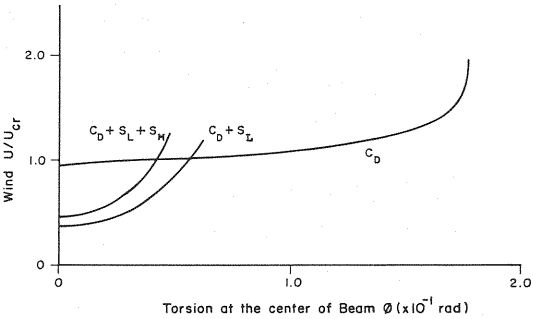


Fig.10 Post Buckling Behavior of a Beam under Wind Forces.

under the constant directional loads<sup>8)</sup>, a general treatment to reflect the displacement-dependency of the loads has been developed here, and the corresponding load stiffness matrices have been expressed in a general manner.

As important examples, firstly, the well-known problem of a cantilever subjected to the follower force has been examined, and its explicit expression of the load stiffness matrix is given. Secondly, rather important in this paper, the load stiffness matrix of wind forces acting on spatial thin-walled members has been derived explicitly in a concise form. Since both of the load stiffness matrices derived are found nonsymmetric, indicating the nonconservativeness of the load, the dynamic stability becomes of great concern and thus the mass matrix of spatial thin-walled members is also derived in this study to examine its possibility.

The methods of analysis presented in this paper have been of four types : (1) static instability analysis called divergence, (2) dynamic instability analysis called flutter, (3) static nonlinear finite displacement analysis, and (4) static linearized finite displacement analysis, all of which feature part of the important roles to investigate the stability and post-buckling nonlinear behavior of thin-walled structural systems subjected to displacement-dependent loadings.

Finally, some computational illustrative examples have been given to demonstrate the problems of interest both for the follower force and wind forces, and some interesting characteristics of the instability phenomena and the nonlinear finite displacement behavior are presented for thin-walled members. It has been proved through computations that the analysis methods presented in this paper are reliable, versatile, and easy to handle for practical implementations. It is also worthwhile to note that the treatise of the linearized finite displacement analysis is very simple, but accurate in the vicinity of buckling point which seems a primary region of interest for practical applications.

## ACKNOWLEDGEMENTS

This study is supported in part by the Grant in Aid for Scientific Research from the Japanese Ministry of Education, Science and Culture. Thanks are also due to Mr. Prakash Shrestha, Research Associate of the Asian Institute of Technology, for his help to finalize the preparation of manuscript.

## REFERENCES

- 1) Bolotin, V. V. : *Nonconservative Problems of the Theory of Elastic Stability*, Pergamon Press, Oxford, 1963.
- 2) Bolotin, V. V. : *The Dynamic Stability of Elastic Systems*, Holden-Day, San Francisco, 1964.
- 3) Huseyin, K. : *Nonlinear Theory of Elastic Stability*, Noordhoff, Leyden, 1974.
- 4) Huseyin, K. : *Vibrations and Stability of Multiple Parameter Systems*, Noordhoff, Alphen, 1978.
- 5) Argyris, J.H. and Symeonidis, Sp. : *Nonlinear Finite Element Analysis of Elastic Systems Under Nonconservative Loadings-Natural Formulation*, *Comp. Meths. Appl. Mech. Eng.* 26, pp.75~123, 1981.
- 6) Schweizerhof, K. and Ramm, E. : *Displacement Dependent Pressure Loads in Nonlinear Finite Element Analysis*, *Computers and Structures*, Vol.18, No.6, pp.1099~1114, 1984.
- 7) Bufler, H. : *Pressure Loaded Structures Under Large Deformations*; *ZAMM*, 64, pp.287~295, 1984.7.
- 8) Hasegawa, A., Liyanage, K., Ikeda, T. and Nishino, F. : *A Concise and Explicit Formulation of Out-of-Plane Instability of Thin-Walled Members*, *Structural Engineering/Earthquake Engineering*, Vol.2, No.1, pp.57s~65s, Apr.1985 (*Proc. JSCE*, No.356/I-3).
- 9) Timoshenko, S.P. and Gere, J.M. : *Theory of Elastic Stability*, 2nd ed.; McGraw-Hill, New York, pp.152~156, 1961.
- 10) Hirai, A. : *Steel Bridges III*, Gihodo Publishing Co., Tokyo, 1956 (in Japanese).
- 11) Hasegawa, A., Liyanage, K.K. and Nishino, F. : *A Non-iterative Nonlinear Analysis Scheme of Frames with Thin-Walled Elastic Members*, *Structural Engineering/Earthquake Engineering*, Vol.4, No.1, Apr.1987, pp.19s-29s (*Proc. JSCE*, No.380/I-7)

(Received June 8 1987)